Bioorganic & Medicinal Chemistry Letters 22 (2012) 4645–4649

Contents lists available at SciVerse ScienceDirect

Bioorganic & Medicinal Chemistry Letters

journal homepage: www.elsevier.com/locate/bmcl

# Structure-based optimization of aminopyridines as PKCθ inhibitors

Juan-Miguel Jimenez [a,*], Christopher Davis [a,*], Dean Boyall [a], Damien Fraysse [a], Ronald Knegtel [a], Luca Settimo [a], Stephen Young [a], Claire Bolton [b], Peter Chiu [b], Adam Curnock [b], Richele Rasmussen [b,†], Adam Tanner [b], Ian Ager [b]

[a] Department of Chemistry at Vertex Pharmaceuticals (Europe) Ltd, 88 Milton Park, Abingdon OX14 4RY, United Kingdom
[b] Department of Biology at Vertex Pharmaceuticals (Europe) Ltd, 88 Milton Park, Abingdon OX14 4RY, United Kingdom

ARTICLE INFO

*Article history:*
Received 25 April 2012
Revised 22 May 2012
Accepted 24 May 2012
Available online 6 June 2012

*Keywords:*
PKCθ
Kinase
SEB-IL2
Aminopyridine
T cell receptor

ABSTRACT

The identification of a novel series of PKCθ inhibitors and subsequent optimization using docking based on a crystal structure of PKCθ is described. SAR was rapidly generated around an amino pyridine-ketone hit; (6-aminopyridin-2-yl)(2-aminopyridin-3-yl)methanone **2** leading to compound **21** which significantly inhibits production of IL-2 in a mouse SEB-IL2 model.



Protein kinase C theta (PKCθ) is a member of a large family of serine/threonine kinases that are involved in a diverse range of cellular functions. There are 11 PKC isoforms that can be sub-divided into DAG- and calcium-dependent, classical isoforms (PKCs α, βI, βII and γ) DAG-dependent, novel isoforms (PKCs δ, ε, η and θ) and DAG- and calcium-independent atypical isoforms (PKCs λ, ι and ζ).[1]

PKCθ plays a central role in the activation of T cells and integrates signals from both the T cell receptor (TCR) and the co-stimulatory CD28. During T cell activation, PKCθ is recruited to the center of the immune synapse (IS) and is responsible for the activation of key transcription factors, AP-1, NFκB and NFAT that drive transcription of the IL-2 gene, an essential step in T cell activation.[2] Importantly, studies in PKCθ knockout mice have demonstrated that whilst antiviral responses are PKCθ independent, T-cell responses associated with autoimmune diseases are PKCθ dependent.[3,4] Consequently, it is anticipated that a selective PKCθ inhibitor will provide the desired balance of efficacy and safety for the treatment of autoimmune diseases.

Novartis' pan-PKC inhibitor, AEB071 (Sotrastaurin) **1**, is currently in phase II clinical studies for transplantation, ulcerative colitis and psoriasis.[5] AEB071 is a potent inhibitor of classical and novel PKC isoforms and is a potent inhibitor of the isoforms involved in B cell and T cell function, PKCα, PKCβ and PKCθ.

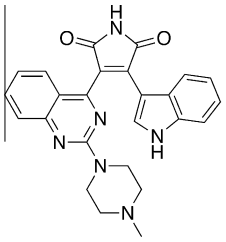

Sotrastaurin (AEB071, **1**)

There has been significant interest in the development of PKCθ selective inhibitors for the treatment of autoimmune diseases and there are several companies with small molecule PKCθ inhibitor programs.[6–18] Whilst some have reported promising pre-clinical data, to date, there are no selective PKCθ inhibitors confirmed to be in the clinic.

The aim of our program was to identify potent and selective PKCθ inhibitors to provide safer options to treat autoimmune diseases. Compound **2,** (2-aminopyridine-3-yl)(6-(1,4-diazepan-1-yl)pyridine-2-yl)methanone was one of the most promising hits during

* Corresponding authors. Tel./fax: +44 1235 438800.
*E-mail addresses:* juan-miguel_jimenez@vrtx.com (J.-M. Jimenez), chris_davis@vrtx.com (C. Davis).
† Present address: National Health and Medical Research Council, GPO Box 1421, Canberra, ACT 2601, Australia.

0960-894X/$ - see front matter © 2012 Elsevier Ltd. All rights reserved.
http://dx.doi.org/10.1016/j.bmcl.2012.05.114

our HTS campaign. It is a potent inhibitor of PKCθ ($K_i$ = 164 nM) with good selectivity over other kinases outside the PKC family.

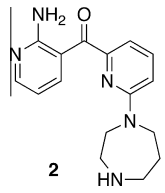

**2**

PKCθ Ki = 164 nM
cLogP = 2
PSA = 84
LLE = 4.8
LE = 0.3

In addition to the favorable inhibition profile, compound **2** shows desirable features, such as low molecular weight (297.16), low calculated polar surface area (84), calculated LogP of 2, good permeability (Caco-2 A–B $9 \times 10^{-6}$ cm/s, B–A $11 \times 10^{-6}$ cm/s) and high ligand and lipophilic efficiency (LE and LLE)[19] (0.3 and 4.8). Compound **2** was considered an excellent starting point for our optimization efforts. Our first objective was to improve the PKCθ potency of compound **2**.

Using docking and minimization of **2** in PKCθ,[20–22] the compound is predicted to bind to the hinge region of PKCθ via the aminopyridine with the ketone pointing towards the gatekeeper region and potentially making an interaction with Thr442. The NH of the 1,4-diazepane is predicted to make an interaction with the main chain carbonyl oxygen atom of Asp508 (Fig. 1). In addition, docking and minimization of **2** in PKCθ also suggests that there are two main areas of the PKCθ active site where lipophilic interactions could provide the desired increase in potency; region A targeting the C-terminus region and region B targeting the 'back pocket' near the gatekeeper (Fig. 1).

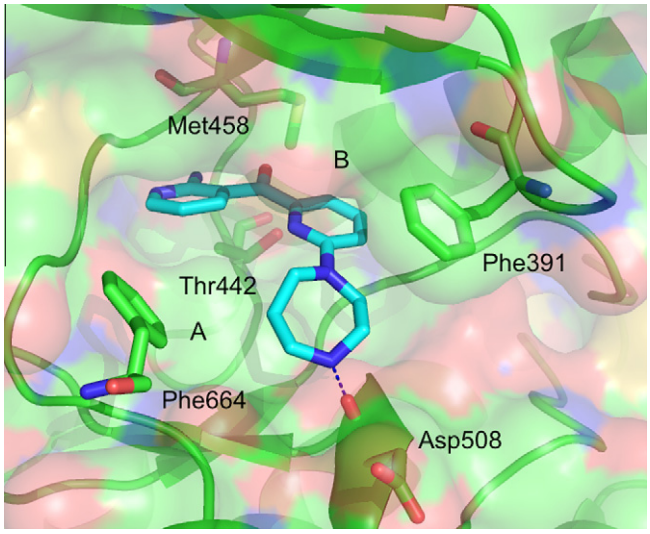


**Figure 1.** Docking and minimization of compound **2** in the active site of PKCθ, showing the two regions to be investigated.

**Table 1**
Effect of amine ring size and positioning of amine

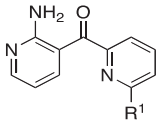

| Compounds | $R^1$ | PKCθ $K_i$[a] (μM) | *c*Log*P*<br>LLE<br>LE | Compounds | $R^1$ | PKCθ $K_i$[a] (μM) | *c*Log*P*<br>LLE<br>LE |
|---|---|---|---|---|---|---|---|
| **2** | 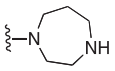 | 0.164[b] | 2.0<br>4.8<br>0.3 | **7** | 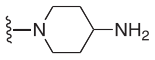 | 0.076 | 1.7<br>5.4<br>0.3 |
| **3** | 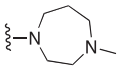 | 0.375 | 2.4<br>4.0<br>0.3 | **8** | 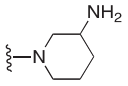 | 1.975 | 2.2<br>3.5<br>0.3 |
| **4** | 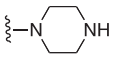 | 0.032[b] | 2.0<br>5.5<br>0.4 | **9** | 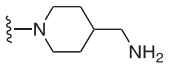 | 1.39 | 2.2<br>3.7<br>0.3 |
| **5** | 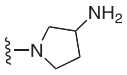 | 1.52 | 1.7<br>4.2<br>0.3 | **10** | 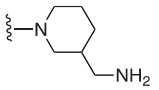 | >2.8 | 2.2<br>ND<br>ND |
| **6** | 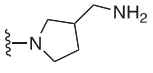 | 0.745 | 1.8<br>4.4<br>0.3 | **11** | 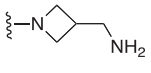 | 1.01 | 1.6<br>4.4<br>0.3 |

[a] Mean from *n* values of 2 independent experiments.
[b] Mean from *n* = 6.

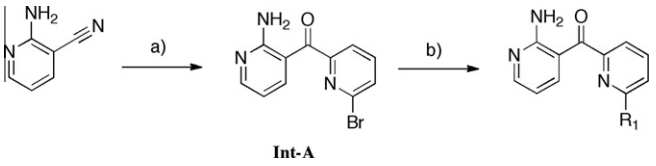


**Scheme 1.** Reagents and conditions: (a) (i) 2,6-Dibromopyridine, <−30 °C, (ii) BuLi 2.5 M in hexanes, <30 °C; (b) amine, $K_2CO_3$, DMF, 110 °C.

In order to allow rapid optimization of these interactions, a key intermediate **A** was synthesised from the commercially available 2-aminonicotinonitrile as shown in Scheme 1. This intermediate was prepared by a 'one pot' anion formation and nucleophilic addition reaction giving **Int-A**, (2-aminopyridin-3-yl)(6-bromo pyridin-2-yl) methanone in 50% yield.

An initial set of amines was then synthesized via displacement of 6-bromopyridine intermediate **Int-A** and are shown in Table 1. The SAR generated shows that the original 1,4-diazepane was actually fairly close to optimum with only the piperazine **4** showing a significant increase (fivefold) in PKCθ activity. Methylation of the 1,4-diazepane NH present in compound **2**, $K_i$ = 164 nM, causes an approximately twofold loss in PKCθ activity, as shown by compound **3**, $K_i$ = 375 nM. From this amine set, piperazine, **4**, was chosen for further optimization due to its greater PKCθ activity and ligand efficiency.

To improve further the PKCθ activity of compound **4** we postulated that a lipophilic interaction could be made between the C-3 position of the piperazine and region A of the PKCθ active site. To explore this further, a set of substituted piperazines were prepared with a diverse range of lipophilic substitutents as shown in Table 2.

Addition of an (*S*-)-methyl group, **12**, showed little change in activity with a PKCθ $K_i$ of 67 nM. Extending the lipophilicity to an isopropyl group **15** or to isobutyl group **18** showed increasing activity whilst maintaining a good level of lipophilic efficiency with PKCθ $K_i$'s of 4 nM and 3 nM respectively. The PKCθ activity is very sensitive to the stereochemistry at this C-3 position, with the *S*-enantiomer being over 35-fold more potent than the *R*-enantiomer, as shown by the enantiomeric pairs **19** & **20** and **15** & **16**. Disubstitution at the C-3 position of the piperazine ring, compound

**Table 2**
Effect of piperazine substitution on PKCθ activity

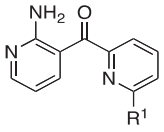


| Compounds | $R^1$ | PKCθ $K_i$[a] (μM) | *c*Log*P*<br>LLE<br>LE | Compounds | $R^1$ | PKCθ $K_i$[a] (μM) | *c*Log*P*<br>LLE<br>LE |
|---|---|---|---|---|---|---|---|
| **4** | 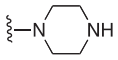 | 0.032 | 2.0<br>5.5<br>0.4 | **16** | 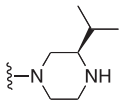 | 0.275 | 3.3<br>3.3<br>0.3 |
| **12** | 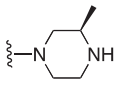 | 0.182 | 2.4<br>4.8<br>0.3 | **17** | 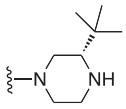 | 0.038 | 3.7<br>3.8<br>0.3 |
| **13** | 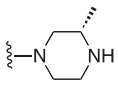 | 0.067 | 2.4<br>4.4<br>0.3 | **18** | 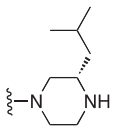 | 0.003 | 3.7<br>4.9<br>0.3 |
| **14** | 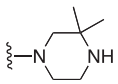 | 0.085 | 2.7<br>4.4<br>0.3 | **19** | 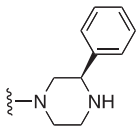 | 0.238 | 3.8<br>2.9<br>0.2 |
| **15** | 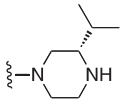 | 0.004 | 3.3<br>5.3<br>0.4 | **20** | 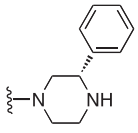 | 0.006 | 3.8<br>4.5<br>0.3 |

[a] Mean from $n \geqslant 2$ independent experiments.

**Table 3**
Effect of pyridine substitution of 3- or 4- position on PKCθ activity and kinase selectivity

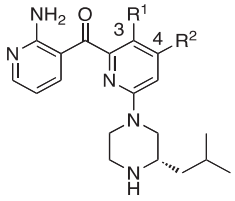

| Compounds | $R^1$ | $R^2$ | PKCθ $K_i$[a] (μM) | PKCδ $K_i$[a] (μM) | PKCα $K_i$[a] (μM) | IL-2 Cell $IC_{50}$[b] (μM) | Kinases-fold selectivity[b] |
|---|---|---|---|---|---|---|---|
| **18** | H | H | 0.003 | 0.020 | 0.054 | 0.165 | Src >1400 PKA 60 Gsk3b 143 |
| **21** | $CF_3$ | H | 0.003 | 0.037 | 0.076 | 0.052 | Src >1300 PKA 47 Gsk3b 400 |
| **22** | Cl | H | 0.002 | 0.022 | 0.049 | 0.058 | Src >4000 PKA 38 Gsk3b 255 |
| **23** | Cyclopropyl | H | 0.028 | 0.255 | 2.65 | 2.6 | Src >140 PKA 93 Gsk3b >140 |
| **24** | $F_2HCO$ | H | 0.007 | 0.087 | 0.459 | 0.229 | Src >570 PKA 84 Gsk3b >570 |
| **25** | $CF_3CH_2O$ | H | 0.29 | 1.3 | >1.25 | ND | Src >13 PKA >13 Gsk3b >13 |
| **26** | Propyl | H | 0.02 | 0.03 | 1.23 | 0.41 | Src >200 PKA 24 Gsk3b >200 |
| **27** | Ph | H | 0.0006 | <0.01 | 0.01 | 0.005 | Src 10 PKA 3 Gsk3b 30 |
| **28** | Benzyl | H | >0.7 | >2 | >1.25 | ND | Src ND PKA ND Gsk3b ND |
| **29** | H | Me | 0.024 | 0.116 | 0.459 | 0.41 | Src >167 PKA 7 Gsk3b 18 |

[a] Mean from $n \geqslant 2$ independent experiments.
[b] Data from $n = 1$.

**Table 4**
Extended selectivity profile of compound **21**

| Enzymes in TCR pathway $IC_{50}$[a] (μM) | Lck >2 | Itk >2 | Fyn >2 | Lyn >2 | Zap70 >2 | c-Raf >2 | Erk-1 >2 |
|---|---|---|---|---|---|---|---|
| | Syk >4 | Jak2 >4 | | Rock1 >4 | | Flt3 0.580 | PI3 kγ >4 |
| Other kinases $K_i$[a] (μM) | PKCβ 0.260 | PKCε 0.017 | | Met >4 | | PI3 Kα >4 | CdK2 >4 |
| | Kdr >4 | PIk >4 | | Jnk3 >4 | | | |

[a] Data from $n = 1$ independent experiments.

**Table 5**
Mouse PK for compound **21** (IV-bolus dose 3 mg/kg and PO dose of 10 mg/kg). Data reported as an average of three animals.

| Cl (mL/min/kg) | $T_{1/2}$ (h) | Vz (L/kg) | VSS (L/kg) | MRT (h) | %F |
|---|---|---|---|---|---|
| 203 | 1.3 | 19.7 | 15.8 | 1.4 | 45 |

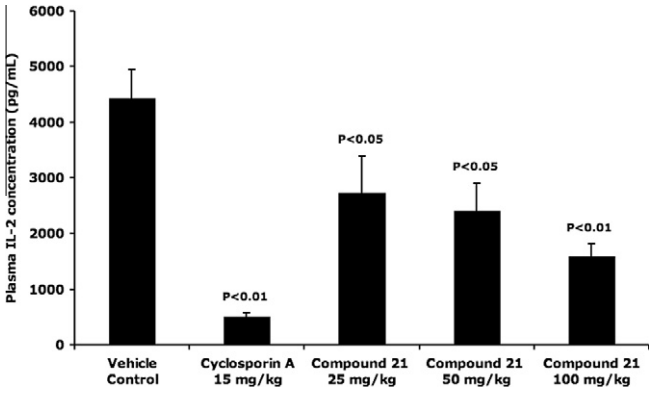


**Figure 2.** Mouse SEB-IL2 dose response to PO dosing of compound **21**.

**14**, showed no gain in PKCθ potency as compared with mono substituted, **13**, or unsubstituted, **4** but is less efficient in terms of LE and LLE.

Compound **18**, containing the (*S*-)-isobutyl piperazine, was selected for further optimisation due to its high level of PKCθ inhibitory activity. Based on our models of compound **18** in PKCθ, we also wanted to fill region B near the gatekeeper residue in order to gain further PKCθ activity. Our predicted binding mode suggested that we could target this area by substitution from the C3 or C4 position of the central pyridine ring. A set of compounds was made to explore this region of the active site as shown in Table 3.

Addition of a phenyl ring, as in compound **27**, showed exquisite PKCθ potency with a $K_i$ of 0.6 nM but also proved to be less selective over other kinases than most other compounds in the series. Unfortunately, compound **27** showed unacceptable levels of cytotoxicity (data not shown). Saturated alkyl groups in this region were detrimental to PKCθ activity, such as propyl **26** and cyclopropyl **23** with $K_i$'s of 20 and 28 nM respectively. Addition of a $CF_3$ group (**21**) (LE = 21, LLE = 4.0) or Cl (**22**) (LE = 23, LLE = 4.5) showed no effect on PKCθ activity but at a loss of ligand and lipophilic efficiency as compared with H (**18**) (LE = 25, LLE = 4.9), while maintaining a good level of cellular potency and kinase selectivity (see Table 3). However, they did improve the PK characteristics; providing greater oral exposure and longer $t_{1/2}$ in rat. Consequently, compound **21** was selected for in vivo assessment on the basis of its overall profile. Good PKCθ potency ($K_i$ = 0.003 μM) translated to good cell activity (IL-2 $IC_{50}$ 0.052 μM) and excellent overall kinase selectivity (see Table 4). Although mouse PK of **21** was far from ideal (Table 5), it was deemed suitable to test in our mouse SEB-IL2 model (see Fig. 2).[23]

Compound **21** was dosed once orally at 25, 50 and 100 mg/kg in our mouse SEB-IL2. These data showed that **21** significantly inhibited the production of IL-2 in a dose dependent manner (Fig. 2). The level of efficacy observed in vivo is in line with the free concentration achieved at the doses tested (e.g., at 100 mg/kg C-max free concentration is 150 nM). The mechanism for this IL-2 inhibition

is driven by PKCθ inhibition of **21**, as the other kinases in the TCR signaling pathway are not inhibited, as shown in Table 4.

In summary, we have described the synthesis and biological evaluation of a series of (6-aminopyridin-2-yl)(2-aminopyridin-3-yl)methanone as PKCθ inhibitors. The program started with the identification of hit **2** and subsequent optimization with the aid of docking and minimization in PKCθ, which led to the discovery of **21**. Compound **21** is a potent inhibitor of PKCθ, which displayed modest selectivity over closely related members of the PKC novel subfamily and excellent selectivity across broad kinase space. The compound shows activity in cellular and in vivo assays that measures the functional activity of PKCθ. The efforts to improve further on the PKC isoform selectivity and PK characteristics will be reported in due course.

## Acknowledgement

The authors thank Don Middleton for his valuable assistance.

## Supplementary data

Supplementary data associated with this article can be found, in the online version, at http://dx.doi.org/10.1016/j.bmcl.2012.05.114.

## References and notes

1. Rosse, C.; Linch, M.; Kermorgant, S.; Cameron, A. J.; Boeckeler, K.; Parker, P. J. *Nat. Rev. Mol. Cell Biol.* **2010**, *11*, 103.
2. Manicassamy, S.; Sadim, M.; Ye, R. D.; Sun, Z. *J. Mol. Biol.* **2006**, *355*, 347 and references herein.
3. Marsland, B. J.; Soos, T. J.; Spath, G.; Littman, D. R.; Kopf, M. *J. Exp. Med.* **2004**, *200*, 181.
4. Giannoni, F.; Lyon, A. B.; Wareing, M. D.; Dias, P. B.; Sarawar, S. R. *J. Virol.* **2005**, *79*, 6808.
5. Wagner, J.; Matt, P. V.; Faller, B.; Cooke, N. G.; Albert, R.; Sedrani, R.; Wiegand, H.; Jean, C.; Beerli, C.; Weckbecker, G.; Evenou, J.-P.; Zenke, G.; Cottens, S. *J. Med. Chem.* **2011**, *54*, 6028.
6. Subrath, J.; Wang, D.; Wu, B.; Niu, C.; Boschelli, D. H.; Lee, J.; Yang, X.; Brennan, A.; Chaudhary, D. *Bioorg. Med. Chem. Lett.* **2009**, *19*, 5423.
7. Prashad, A. S.; Wang, D.; Subrath, J.; Wu, B.; Lin, M.; Zhang, M. Y.; Kagan, N.; Lee, J.; Yang, X.; Brennan, A.; Chaudhary, D.; Xu, X.; Leung, L.; Wang, J.; Boschelli, D. H. *Bioorg. Med. Chem. Lett.* **2009**, *19*, 5799.
8. Cole, D. C.; Asselin, M.; Brennan, A.; Czerwinski, R.; Ellingboe, J. W.; Fitz, L.; Greco, R.; Huang, X.; Joseph-McCarthy, D.; Kelly, M. F.; Kirisits, M.; Lee, J.; Li, Y.; Morgan, P.; Stock, J. R.; Tsao, D. H.; Wissner, A.; Yang, X.; Chaudhary, D. *J. Med. Chem.* **2008**, *51*, 5958.
9. Dushin, R. G.; Nittoli, T.; Ingalls, C.; Boschelli, D. H.; Cole, D. C.; Wissner, A.; Lee, J.; Yang, X.; Morgan, P.; Brennan, A.; Chaudhary, D. *Bioorg. Med. Chem. Lett.* **2009**, *19*, 2461.
10. Wu, B.; Boschelli, D. H.; Lee, J.; Yang, X.; Chaudhary, D. *Bioorg. Med. Chem. Lett.* **2009**, *19*, 766.
11. Boschelli, D. H.; Wu, B.; Barrios Sosa, A. C.; Chen, J.; Asselin, M.; Cole, D. C.; Lee, J.; Yang, X.; Chaudhary, D. *Bioorg. Med. Chem. Lett.* **2008**, *18*, 2850.
12. Nathan Tumey, L.; Boschelli, D. H.; Lee, J.; Chaudhary, D. *Bioorg. Med. Chem. Lett.* **2008**, *18*, 4420.
13. Boschelli, D. H.; Wang, D.; Prashad, A. S.; Subrath, J.; Wu, B.; Niu, C.; Lee, J.; Yang, X.; Brennan, A.; Chaudhary, D. *Bioorg. Med. Chem. Lett.* **2009**, *19*, 3623.
14. Boschelli, D. H.; Subrath, J.; Niu, C.; Wu, B.; Wang, Y.; Lee, J.; Brennan, A.; Ho, M.; Deng, B.; Yang, X.; Xu, X.; Leung, L.; Wang, J.; Atherton, J.; Chaudhary, D. *Bioorg. Med. Chem. Lett.* **1965**, *2010*, 20.
15. Niu, C.; Boschelli, D. H.; Tumey, L. N.; Bhagirath, N.; Subrath, J.; Shim, J.; Wang, Y.; Wu, B.; Eid, C.; Lee, J.; Yang, X.; Brennan, A.; Chaudhary, D. *Bioorg. Med. Chem. Lett.* **2009**, *19*, 5829.
16. Shim, J.; Eid, C.; Lee, J.; Liu, E.; Chaudhary, D.; Boschelli, D. H. *Bioorg. Med. Chem. Lett.* **2009**, *19*, 6575.
17. Cywin, C. L.; Dahmann, G.; Prokopowicz, A. S., 3rd; Young, E. R.; Magolda, R. L.; Cardozo, M. G.; Cogan, D. A.; Disalvo, D.; Ginn, J. D.; Kashem, M. A.; Wolak, J. P.; Homon, C. A.; Farrell, T. M.; Grbic, H.; Hu, H.; Kaplita, P. V.; Liu, L. H.; Spero, D. M.; Jeanfavre, D. D.; O'shea, K. M.; White, D. M.; Woska, J. R., Jr.; Brown, M. L. *Bioorg. Med. Chem. Lett.* **2007**, *17*, 225.
18. Boschelli, D. H. *Curr. Top. Med. Chem.* **2009**, *9*, 640.
19. Ligand efficiency LE = p$K_i$/heavy atom count. Lipophilic ligand efficiency LLE = p$K_i$−*c* Log *P*.
20. Based on the published PKCtheta crystal stucture from Novartis: Rummel, G.; Stark, W.; Strauss, A.; Wagner, J. PCT Int. Appl. WO2004076654, 2004.
21. Novartis PKCθ crystal structure available from RCSB protein data bank, accession code: 2JED.
22. For docking methods refer to Supplementary data.
23. For full details regarding the SEB-IL2 pharmacology model, refer to Supplementary data.